

Computing the free energy of molecular solids by the Einstein molecule approach: Ices XIII and XIV, hard-dumbbells and a patchy model of proteins

E. G. Noya, M. M. Conde and C. Vega*

*Departamento de Química-Física, Facultad de Ciencias Químicas,
Universidad Complutense de Madrid, E-28040 Madrid, Spain*

(Dated: October 22, 2018)

Abstract

The recently proposed Einstein molecule approach is extended to compute the free energy of molecular solids. This method is a variant of the Einstein crystal method of Frenkel and Ladd[J. Chem. Phys. **81**, 3188 (1984)]. In order to show its applicability, we have computed the free energy of a hard-dumbbells solid, of two recently discovered solid phases of water, namely, ice XIII and ice XIV, where the interactions between water molecules are described by the rigid non-polarizable TIP4P/2005 model potential, and of several solid phases that are thermodynamically stable for an anisotropic patchy model with octahedral symmetry which mimics proteins. Our calculations show that both the Einstein crystal method and the Einstein molecule approach yield the same results within statistical uncertainty. In addition, we have studied in detail some subtle issues concerning the calculation of the free energy of molecular solids. First, for solids with non-cubic symmetry, we have studied the effect of the shape of the simulation box on the free energy. Our results show that the equilibrium shape of the simulation box must be used to compute the free energy in order to avoid the appearance of artificial stress in the system that will result in an increase of the free energy. In complex solids, such as the solid phases of water, another difficulty is related to the choice of the reference structure. As in some cases there is not an obvious orientation of the molecules, it is not clear how to generate the reference structure. Our results will show that, as long as the structure is not too far from the equilibrium structure, the calculated free energy is invariant to the reference structure used in the free energy calculations. Finally, the strong size dependence of the free energy of solids is also studied.

* published in J. Chem. Phys. 129 104704 (2008)

I. INTRODUCTION

Since the pioneering work of Hoover *et al.*,¹ determining the free energy of molecular solids has been an important area of research.^{2,3,4,5,6,7,8} One of the most popular methods to compute the free energy of solids is the Einstein crystal method, proposed by Frenkel and Ladd more than two decades ago.² In this method, the free energy of a given solid is computed by designing an integration path that links the solid to an ideal Einstein crystal with the same structure as the real solid, for which the free energy can be analytically computed. This method was soon extended to molecular solids.³ In this case, in addition to the springs that bound each molecule to its lattice position, springs that keep the particles in the right orientation must also be added.^{3,9} Using this technique, the free energy of several atomic and molecular solids has been computed.^{4,9,10,11,12,13,14,15,16,17,18,19,20,21,22,23,24,25,26,27,28,29,30,31,32,33,34,35,36}

Quite recently a new method to compute the free energies of solids which was denoted as “the Einstein molecule” approach has been proposed.^{37,38} This method consists of a slight modification of the Einstein crystal method. In the Einstein crystal method, the reference system is an ideal Einstein crystal with the constraint that the center of mass of the system is fixed in order to avoid a quasi-divergence in the integral of the free energy change from the real solid to the reference system. This constraint introduces some complexity in the method. In particular, the derivation of some terms that contribute to the free energy is somewhat involved.^{2,39} The main idea behind the Einstein molecule approach is that the derivation of the analytical expressions can be considerably simplified by fixing the position of one molecule instead of fixing the center of mass of the system. The Einstein molecule approach has been successfully applied to compute the free energy of the hard-spheres (HS) and Lennard-Jones (LJ) face centered cubic (fcc) solids. Here it will be shown how it can be applied to molecular solids.

Moreover, even though the Einstein crystal method has been extended to molecular solids more than twenty years ago, there are several subtle issues concerning the calculation of the free energy that are not clear yet. These difficulties are common to the Einstein crystal and Einstein molecule approaches. One of these issues concerns the shape of the simulation box. For solids with non-cubic symmetry, prior to the computation of the free energy for a given thermodynamic state, the solid structure must be relaxed to obtain the equilibrium unit cell corresponding to that thermodynamic state. This is not usually a problem in structures

with cubic symmetry, as the equilibrium structure is determined uniquely by the lattice parameter a . However, in structures with lower symmetry, it is convenient to first perform a simulation in which both the edges and the angles that define the simulation box are allowed to relax to the equilibrium structure. This can be achieved by, previously to the free energy calculation, performing a Parrinello-Rahman NpT simulation. Other alternative would be to perform a simulation at constant volume but where the shape of the simulation box is allowed to change, i. e., a variable-shape constant volume (VSNVT) simulation.^{11,31,40,41} We would like to stress the importance of using the equilibrium structure to compute the free energy, otherwise the solid could be under some stress that will lead to an increase of the free energy. This has already been noted previously,^{3,9} but, due to its importance, we believe that it is worthy to review this point.

Another difficulty that one might encounter when computing the free energy of molecular solids concerns the reference structure that is used either in the Einstein crystal or in the Einstein molecule approaches. In simple solids, in which all the particles exhibit the same orientation, this does not pose a problem, as the reference structure is chosen simply as a solid where all the particles lie on their lattice positions and are perfectly oriented. However, for more complex solids, where not all the molecules exhibit the same orientation, the choice of the reference structure might be a subtle issue. This is the case, for example, of some solid phases of water that exhibit complex unit cells. In this situation several choices are possible. One might choose to build the reference structure by using experimental data to obtain the position and orientation of the molecules or, alternatively, one might choose to perform an energy minimisation, so that each molecule will be located as to minimise the potential energy.⁴² Another reasonable choice would be to calculate the average positions and orientations at the particular thermodynamic state under study. In view of this ambiguity, it is of interest to investigate the effect that one choice or another has on the calculation of the free energy.

Finally, another difficulty arises from the strong size dependence of the free energy of solids. In particular, for the fcc HS solid, several authors have shown that the free energy per particle decreases linearly with $1/N$, N being the number of particles in the system.^{34,37,39} As a consequence, the fluid-solid coexistence point also exhibits a strong size dependence (note that the finite size effects on the free energy of the fluid and on the equation of state of both phases must also be considered). The size dependence of the fluid-solid coexistence

point obtained with the values of the free energy from those works³⁷ is in agreement with the coexistence points calculated by Wilding and Bruce^{43,44} using a completely different route, the phase-switch Monte Carlo method.^{45,46,47} This strong size dependence has also been observed for other systems, such as for example, the fcc LJ solid.^{37,48} In this case, the situation is more complicated because, in addition to the size dependence of the free energy, there is also a dependence on the cutoff of the potential. Both effects must be studied separately.³⁷ This means that in order to perform a rigorous calculation of the free energy of a given solid, the free energy must be computed for different system sizes, so that the value of the free energy at the thermodynamic limit can be obtained by extrapolation to N going to infinity. However, this procedure requires performing many simulations to compute the free energy of a solid at just one thermodynamic state. Therefore, it would be useful to introduce finite size corrections (FSC), i.e., a simple recipe that would allow one to estimate the value of the free energy in the thermodynamic limit from simulations of a system of finite size. In a previous paper, we have proposed several FSC whose performances were assessed for simple atomic models, namely, the HS and LJ model potentials.³⁷ The best performance was obtained by the so-called Asymptotic FSC, in which the free energy in the thermodynamic limit is estimated from the free energy at a finite size N by taking the limit when N tends to infinity in the expression used to compute the free energy. Depending on how this limit was taken, three different variants were proposed, and all of them give quite reasonable estimates of the free energy in the thermodynamic limit. However, these results might not be general and, therefore, it would be of interest to check whether the FSC work well also for molecular solids.

In this paper we will address all these issues concerning the computation of free energy of solids. It is our hope that this will contribute to encourage other authors to compute free energies. The paper will be structured in the following way. First, the recently proposed Einstein molecule approach will be extended to the case of molecular solids and it will be shown that the results obtained for all the solids studied (i.e., a hard-dumbbells solid, a solid made of anisotropic particles with octahedral symmetry and the two recently discovered solid phases of water, ice XIII and ice XIV) are in agreement, within statistical uncertainty, with the results obtained with the Einstein crystal method. Second, the free energy of ices XIII and XIV using the rigid non-polarizable TIP4P/2005 model of water will also be calculated. These calculations will serve to illustrate the importance of obtaining the equilibrium shape

of the simulation box previously to the computation of the free energy and to explore what is the best choice for the reference structure that is used in the computation of the free energy. Finally, we will perform a systematic study of the size dependence of the free energy of several crystalline solids for a simple anisotropic patchy model with octahedral symmetry. The performance of the previously proposed FSC will be assessed for this model.

II. METHOD

A. Model potentials and solid structures

In what follows we will consider several pair potentials, for which the intermolecular potential will be expressed as:

$$U_{sol} = \sum_{i=1}^{N-1} \sum_{j=i+1}^N u_{sol}(i, j) \quad (1)$$

where $u_{sol}(i, j)$ is the intermolecular potential between molecules i and j .

1. Hard-dumbbells

The first model we considered is the hard-dumbbells (HD) model, in which each particle consists of two hard-spheres, each of diameter σ_{HS} , separated by a distance L . The free energy of this model has already been studied previously using the Einstein crystal method^{9,49} and also theoretically using an extension of the Wertheim theory.^{50,51} The possible solid structures for hard-dumbbells have already been discussed in previous works.^{9,49,52} Hard-dumbbells can form a hexagonal lattice by arranging the dumbbells in such a way that each sphere of a dumbbell lies in a hexagonal layer. The dumbbell axis is then tilted from the normal to the layer by an angle equal to $\arcsin(\frac{L}{\sigma_{HS}\sqrt{3}})$. These layers can be stacked as to form a fcc lattice (structure designated as CP1) or a hcp lattice (structure CP2). In these two structures all the dumbbells exhibit the same tilt angle. Another structure can be obtained by stacking the layers in such a way that the tilt angle alternates between adjacent layers (structure designated as CP3). It has been shown that only the CP1 structure is thermodynamically stable (for $L^* = L/\sigma_{HS} > 0.4$).⁴⁹ For values of L^* lower than approximately 0.4, there is a range of pressures for which a plastic fcc crystal is the most stable

phase.^{49,52} Finally, it is also possible to form aperiodic fcc and hcp structures, i.e., structures in which the axis of the hard-dumbbells are not aligned.^{12,51,53} The aperiodic fcc structure becomes thermodynamically stable for values of the elongation L^* close to unity.^{9,49,51,53} As the main purpose is to show that both the Einstein molecule approach and the Einstein crystal method lead to the same value of the free energy, we have chosen to study only the structure designated as CP1 for hard-dumbbells with $L^* = 1$ (for this elongation the CP1 solid is metastable).

2. *The TIP4P/2005 water model. Ices XIII and XIV*

The interaction between water molecules was modelled using a rigid non-polarizable model potential, the TIP4P/2005 water model.⁵⁴ This model is a variant of the TIP4P potential,⁵⁵ in which the water molecule is modelled by one LJ interaction site on the oxygen atom, two positive charges located on the hydrogen atom and a negative charge that is located on the H-O-H bisector. It has been shown that the TIP4P model is able to predict reasonably well the phase diagram of water. It predicts that ice Ih is the most stable solid phase at the normal melting point and it reproduces the densities of the solid phases of water within 2% of the experimental values.⁵⁶ The main failure of this method seems to be a melting point about 40K below the experimental value.^{27,57} It was then clear that the model could be improved and several groups proposed variants of this model. In particular, the TIP4P/Ice model⁵⁸ has been fitted to reproduce the experimental melting point of water and the TIP4P/Ew⁵⁹ and TIP4P/2005⁵⁴ models reproduce the maximum in density at room pressure. Among these models, we have chosen to use the TIP4P/2005 model potential, because it provides a good description of the phase diagram⁵⁴ and also it predicts to good accuracy the density of the solid phases of ice.⁶⁰

In this work, the free energies of two recently discovered solid phases of water, namely ices XIII and XIV,⁶¹ are computed for the first time. Ice XIII is the proton ordered form of ice V. It has a monoclinic unit cell with 28 molecules. Ice XIV is the proton ordered form of ice XII. It has a tetragonal unit cell with 12 molecules. The TIP4P/2005 model has been shown to reproduce reasonably well the densities of these two solid forms of ice.⁶² In the simulations performed in this work the LJ potential was truncated at 8.5 Å for both solid phases. Standard long range corrections were added to the LJ energy.^{63,64} Ewald sums

were used to deal with the long range electrostatic forces. The real part of the electrostatic contribution was also truncated at 8.5 Å. The screening parameter and the number of vectors of reciprocal space considered had to be carefully selected for each crystal phase.^{63,64}

3. Model particles with octahedral symmetry

We also computed the free energy of a patchy model, which has been previously used as a simplified model of globular proteins.^{65,66,67} This model consists of a repulsive core with some attractive sites (patches) on its surface. In particular, we studied model particles with six patches in an octahedral arrangement. The repulsive core is modelled by the LJ repulsive core, while the attractive term is described by the LJ tail modulated by Gaussian functions centred at the positions of each patch. Therefore, the total energy between two particles is described by the following function:

$$u_{patchy}(\mathbf{r}_{ij}, \mathbf{\Omega}_i, \mathbf{\Omega}_j) = \begin{cases} u_{LJ}(r_{ij}) & r_{ij} < \sigma_{LJ} \\ u_{LJ}(r_{ij}) \exp\left(-\frac{\theta_{k_{min},ij}^2}{2\sigma^2}\right) \exp\left(-\frac{\theta_{l_{min},ji}^2}{2\sigma^2}\right) & r_{ij} \geq \sigma_{LJ} \end{cases} \quad (2)$$

where $u_{LJ}(r_{ij})$ is the Lennard-Jones potential, σ is the standard deviation of the Gaussian, $\theta_{k,ij}$ ($\theta_{l,ji}$) is the angle formed between patch k (l) on atom i (j) and the interparticle vector \mathbf{r}_{ij} (\mathbf{r}_{ji}), and k_{min} (l_{min}) is the patch that minimises the magnitude of this angle. Additionally, for computational efficiency, the potential is truncated and shifted using a cutoff distance of $2.5\sigma_{LJ}$.

Using reduced units (i.e., choosing the unit of energy and length as the values of the LJ parameters ε_{LJ} and σ_{LJ}), the only parameter that needs to be specified is the width of the patches σ . In this work, we have chosen $\sigma = 0.3$ rad., as for this value the whole phase diagram has already been studied.⁶⁷ In this previous study, it has been shown that there are several solid phases that are thermodynamically stable, namely, simple cubic (sc), body-centred cubic (bcc), face-centred cubic (fcc) and, at high temperatures, a plastic fcc crystal. In this work, we will compute the free energy of the three orientationally ordered structures (sc, bcc, and fcc) for several system sizes.

B. The Einstein molecule approach for molecular solids

As mentioned in the Introduction, the Einstein molecule approach is a variant of the Einstein crystal method of Frenkel-Ladd² that has been proposed quite recently.³⁷ Analogously to the Frenkel-Ladd method, the free energy is computed by integration to a reference system whose free energy can be computed analytically. The difference is that in the Einstein molecule approach the reference system is not an ideal Einstein crystal, but an ideal Einstein molecule. The Einstein molecule is defined as an Einstein crystal in which one of the particles does not vibrate. The name of Einstein molecule has been chosen by analogy with molecules, where it is common to use one of the atoms to define the position of a molecule, and the vibrational movement of the remaining atoms is given relative to this reference atom. The Einstein molecule approach has been successfully applied to compute the free energy of simple atomic systems (HS and LJ),³⁷ but we will see that it can be easily extended to molecular solids.

We will start by writing the partition function of a molecular system in the canonical ensemble:

$$Q = \frac{q'^N}{N!\Lambda^{3N}} \int \exp[-\beta U(\mathbf{r}_1, \omega_1, \dots, \mathbf{r}_N, \omega_N)] d\mathbf{r}_1 d\omega_1 \dots d\mathbf{r}_N d\omega_N \quad (3)$$

where $\mathbf{r}_i = (x_i, y_i, z_i)$ is the position of the reference point of molecule i in Cartesian coordinates, and ω_i stands for a set of normalised angles (i.e., $\int d\omega_i = 1$) defining the orientation of particle i . $q' = q_r q_v q_e$, where q_r , q_v and q_e are the rotational, vibrational, and electronic partition functions, respectively. Λ is the thermal de Broglie wavelength ($\Lambda = (h^2/(2\pi m k_B T))^{1/2}$). There is some freedom in choosing the reference point of the molecule. It can be chosen as the center of mass or, alternatively, this reference point can be chosen so that all elements of symmetry pass through it (for a more detailed discussion see Ref. 38). We have chosen the reference point to be at the center of the sphere for the octahedral patchy model and for spheric particles, at the center of mass for hard-dumbbells and at the oxygen atom for water.

The intermolecular potential U depends only on the relative distance between the molecules, not on their absolute positions, i.e., it is invariant under translations. This invariance of the system can be used to write the partition function in a more convenient way by performing a change of variables from $(\mathbf{r}_1, \mathbf{r}_2, \dots, \mathbf{r}_N)$ to $(\mathbf{r}_1, \mathbf{r}_2' = \mathbf{r}_2 - \mathbf{r}_1, \dots, \mathbf{r}_N' = \mathbf{r}_N - \mathbf{r}_1)$.

Therefore, Equation 3 can be written:

$$\begin{aligned}
Q &= \frac{q'^N}{N!\Lambda^{3N}} \int d\mathbf{r}_1 \int \exp[-\beta U(\omega_1, \mathbf{r}'_1, \omega_2, \dots, \mathbf{r}'_N, \omega_N)] d\omega_1 d\mathbf{r}'_2 d\omega_2 \dots d\mathbf{r}'_N d\omega_N \\
&= \frac{q'^N}{N!\Lambda^{3N}} \int d\mathbf{r}_1 \kappa
\end{aligned} \tag{4}$$

The integral κ does not depend on the position of particle 1, \mathbf{r}_1 . Therefore, the integration over \mathbf{r}_1 can readily be performed:

$$Q = \frac{q'^N}{N!\Lambda^{3N}} V \kappa \tag{5}$$

For a system of N indistinguishable particles and for a given position of particle 1 there are $(N-1)!$ possible permutations of the remaining $N-1$ particles. The term κ can be evaluated by computing the integral for a given permutation of the particles (κ') and multiplying it by the number of permutations, so that the partition function can be written as:

$$Q = \frac{q'^N}{N!\Lambda^{3N}} V (N-1)! \kappa' = \frac{q'^N}{N\Lambda^{3N}} V \kappa' \tag{6}$$

We will assume that q' has the same value in the two coexisting phases, so that its value does not affect the coexistence point. For simplicity, in what follows, we will assign q' the value unity.

We will extend now the definition of the ideal Einstein molecule to molecular solids. For atomic solids, an ideal Einstein molecule was defined as an ideal Einstein crystal in which one of the particles does not vibrate and acts as reference. For molecular solids, the ideal Einstein molecule is defined as an ideal Einstein crystal in which the reference point of particle 1 is fixed, but rotations of the molecule about this point are allowed. The reference point of particle 1 is called the carrier, because it transports the lattice, i.e., the position of the lattice is uniquely defined by the position of the reference point of particle 1. The lattice can move as a whole over the volume of the simulation box, and its position is defined by the position of the reference point of particle 1. The potential energy of the ideal Einstein molecule is given by:

$$\begin{aligned}
U_{Ein-mol-id} &= U_{Ein-mol-id,t} + U_{Ein,or} \\
U_{Ein-mol-id,t} &= \sum_{i=2}^N u_{Ein-mol-id,t} = \sum_{i=2}^N [\Lambda_E(\mathbf{r}_i - \mathbf{r}_{i0})^2] \\
U_{Ein,or} &= \sum_{i=1}^N u_{Ein,or}
\end{aligned} \tag{7}$$

where \mathbf{r}_{io} is the position of the reference point of molecule i in the reference Einstein solid, while \mathbf{r}_i represents its position in the current configuration. As can be seen in Eq.7, all the particles except particle 1 (which is fixed) are attached to their lattice positions by harmonic springs. An orientational field ($U_{Ein,or}$) that forces the particles to adopt the right orientation is also included (this field acts over all the particles of the system, including particle 1). The orientational field depends on the symmetry of the particles and, thus, an orientational field must be defined for each model potential. The orientational field used for each one of the model potentials that have been studied in this work will be given in Section II C.

The partition function of the ideal Einstein molecule can be obtained by performing the integral κ' for this particular case:

$$\begin{aligned} \kappa'_{Ein-mol-id} &= \left[\int \exp[-\beta\Lambda_E(\mathbf{r} - \mathbf{r}_0)^2] d\mathbf{r} \right]^{(N-1)} \left[\int \exp(-\beta u_{Ein,or}) d\omega \right]^N = \\ &= \left(\frac{\pi}{\beta\Lambda_E} \right)^{3(N-1)/2} Q_{Ein,or} \end{aligned} \quad (8)$$

where $Q_{Ein,or}$ is the orientational partition function, which is usually evaluated numerically (more details are given the Section II C).

The free energy of the ideal Einstein molecule can be obtained by replacing the partition function given by Eq. 8 in Eq. 6:

$$\begin{aligned} \frac{\beta A_{Ein-mol-id}}{N} &= \frac{\beta A_0}{N} = \frac{\beta A_{0,t}}{N} + \frac{\beta A_{0,or}}{N} = -\frac{1}{N} \ln(Q) \\ &= \left[\frac{1}{N} \ln \left(\frac{N\Lambda^3}{V} \right) + \frac{3}{2} \left(1 - \frac{1}{N} \right) \ln \left(\frac{\Lambda^2 \beta \Lambda_E}{\pi} \right) \right] + \left[-\frac{1}{N} \ln(Q_{Ein,or}) \right] \end{aligned} \quad (9)$$

The numeric value of the thermal de Broglie wavelength Λ is irrelevant to compute the coexistence point as long as the same value is used for both coexisting phases. Therefore, we have chosen to assign Λ the value of the characteristic length for each model potential. Thus, for HS $\Lambda = \sigma_{HS}$, for HD $\Lambda = \sigma_{HS}$, for LJ $\Lambda = \sigma_{LJ}$, for water $\Lambda = 1 \text{ \AA}$ and for the patchy model $\Lambda = \sigma_{LJ}$.

In the Einstein molecule approach, the free energy of a given solid is estimated by designing a path from the ideal Einstein molecule (whose free energy can be computed by Eq. 9) to the real solid. This path can be divided into three steps (see Figure 1). In the first step, the ideal Einstein molecule or, what is the same, the position of the reference point of the carrier (molecule 1) is constrained to a given position. In the second step, the ideal

Einstein molecule with fixed molecule 1 is transformed into the real solid with fixed molecule 1. Finally, in the last step, the solid of interest is recovered by removing the constraint over the position of molecule 1. The free energy change that results from the transformation in the first step is given by a term $k_B T \ln(V/\Lambda^3)$, while the third step contributes by a term $-k_B T \ln(V/\Lambda^3)$. The term V comes from the constraint on the position of molecule 1, and the term Λ^3 comes from the constraint on the momentum. Therefore, the contributions to the final free energy of steps one and three cancel out and all what is needed is to compute the free energy change between an ideal Einstein molecule and the real solid, both with the position (but not the orientation) of particle 1 fixed. This free energy change will be computed in two stages. In the first stage we will evaluate the free energy change between the ideal Einstein molecule (there is no interaction between the particles, only the external Einstein crystal field is present) and the interacting Einstein molecule (in which both the springs and the intermolecular potential are present), both with the position of particle 1 fixed, by a perturbative approach:⁶⁸

$$\Delta A_1 = U_{lattice} - k_B T \ln \langle \exp[-\beta(U_{sol} - U_{lattice})] \rangle_{Ein-mol-id}. \quad (10)$$

where U_{sol} is the potential energy of the real solid and $U_{lattice}$ is the potential energy of the frozen lattice (see Ref. 38 for a more detailed discussion). The brackets with the subscript *Ein - mol - id* indicate that the average is performed by sampling the configurations in a system where only the Einstein field is present. In the second stage, the interacting Einstein molecule with fixed molecule 1 is transformed into the real solid with fixed molecule 1, by slowly turning off the springs, according to the following expression:

$$U(\lambda) = \lambda U_{sol} + (1 - \lambda)(U_{Ein-mol-id} + U_{sol}) \quad (11)$$

where λ is a parameter that takes values between 0 and 1. The free energy change corresponding to this transformation can be estimated by numerically evaluating the following integral:

$$\Delta A_2 = - \int_0^{\Lambda_E} \frac{\langle U_{Ein-mol-id} \rangle_{N,V,T,\lambda}}{\Lambda_E} d(\lambda \Lambda_E). \quad (12)$$

This integral is usually performed by using a Gauss-Legendre quadrature formula. For that purpose, the integrand of this expression must be evaluated at several values of $\lambda \Lambda_E$, which can be done by performing *NVT* MC simulations for those values of the coupling parameter.

Taking all the contributions together, the free energy of solid can be computed as:

$$A_{sol} = A_{Ein-mol-id} + \Delta A_1 + \Delta A_2 \quad (13)$$

which is the central result of this work.

An alternative proof of the Einstein molecule approach can be found in the Appendix. We show that the Einstein molecule method can be obtained as the limit case of the Einstein crystal method when the mass of molecule 1 is much larger than the mass of the remaining molecules.

C. Free energy of the orientational field

We have said before that the orientational field must be chosen so that it has the same symmetry as the molecules. In this section, the orientational fields used for each of the studied model potentials are given. In particular, for hard-dumbbells ($D_{\infty,h}$ symmetry), we have chosen the orientational field:⁹

$$U_{Ein,or} = \sum_{i=1}^N [\Lambda_{E,b} \sin^2(\psi_{b,i})]. \quad (14)$$

where $\psi_{b,i}$ is the angle formed between the axis of particle i and the equilibrium position of the axis of particle i in the CP1 HD solid. In this case, the partition function of the orientational field can be computed as:

$$Q_{Ein,or} = \left[\frac{1}{4\pi} \int \exp(-\beta \Lambda_{E,b} \sin^2(\psi_{b,i})) \sin\theta d\theta d\phi \right]^N \quad (15)$$

where θ and ϕ are the polar angles that define the orientation of the axis of the molecule. In this case, the angle $\psi_{b,i}$ can be identified with the polar angle θ . Therefore, this expression can be simplified to the following integral in one dimension:

$$Q_{Ein,or} = \left[\int_0^1 \exp[\beta \Lambda_{E,b}(x^2 - 1)] dx \right]^N \quad (16)$$

This integral can be evaluated using a numerical integration method, such as, for example, the Simpson's rule.

The water molecule exhibits C_{2v} symmetry and, therefore, a convenient choice of the orientational field is:⁴

$$U_{Ein,or} = \sum_{i=1}^N \left[\Lambda_{E,a} \sin^2(\psi_{a,i}) + \Lambda_{E,b} \left(\frac{\psi_{b,i}}{\pi} \right)^2 \right]. \quad (17)$$

In this case, the orientation of the molecule is defined by two unitary vectors, \vec{a} and \vec{b} . These vectors are obtained as the subtraction (\vec{a}) and the addition (\vec{b}) of the two hydrogen vectors given relative to the position of the oxygen atom. The angle $\psi_{a,i}$ is the angle formed by the vector \vec{a} of molecule i in a given configuration (\vec{a}_i) and the vector \vec{a} in the reference configuration ($\vec{a}_{i,0}$) of the external Einstein field. $\psi_{b,i}$ is defined analogously but with vector \vec{b} (for further details see Ref. 38). The orientational partition function can be computed as:

$$Q_{Ein,or} = \left[\frac{1}{8\pi^2} \int \exp \left(-\beta \left\{ \Lambda_{E,a} \sin^2(\psi_a) + \Lambda_{E,b} \left(\frac{\psi_b}{\pi} \right)^2 \right\} \right) \sin\theta d\theta d\phi d\chi \right]^N \quad (18)$$

where θ , ϕ and χ are the Euler angles that define the orientation of the molecule. This integral can be simplified by choosing the vector \vec{b}_0 as the z axis, so that the Euler angle θ is identical to the vector ψ_b . It can be evaluated numerically by using a Monte Carlo integration method. The efficiency of the Monte Carlo integration method can be considerably improved by realizing that, for large values of $\Lambda_{E,b}$, the exponential decays very rapidly to zero as the angle θ increases, i.e., as the particle rotates away from the reference orientation. Therefore, much efficiency is gained by sampling only small values of θ . We have chosen to sample $\cos\theta$ and only those angles for which the cosine is between 0.99 and 1 have been considered. About 5000×10^6 MC cycles were used to evaluate this integral. In a previous paper, it has been shown that some approximations can be made to this integral for large values of the coupling parameter.⁴ We have found that, for a coupling parameter $\Lambda_{E,a}/(k_B T) = \Lambda_{E,b}/(k_B T) = 25000$, the approximation gives a value for the free energy of the orientational field, $A_{Ein,or}/(Nk_B T) = -1/N \ln(Q_{Ein,or})$, about 0.04 lower than that obtained by performing the exact integral using the Monte Carlo integral method. In particular, using the exact integral we obtained that $A_{Ein,or}/(Nk_B T) = 16.05$, while using the approximate formula, we obtained that $A_{Ein,or}/(Nk_B T) = 16.01$. Although this difference is not too large, we recommend to use the exact expression of the integral, using a numerical algorithm to evaluate it.

As with regard to the patchy model with octahedral symmetry (point group O_h), the orientational field was:⁶⁷

$$U_{Ein,or} = \sum_{i=1}^N \left[\Lambda_{E,a} \sin^2(\psi_{a,i,min}) + \Lambda_{E,b} \sin^2(\psi_{b,i,min}) \right]. \quad (19)$$

where $\psi_{a,i,min}$ is the minimum angle formed by any of the vectors that define the position of the patches in the particle's reference system with respect to the x axis of a fixed reference

system and $\psi_{b,i,min}$ is the analogous quantity with respect to the y axis, where the fixed reference system has been chosen to be coincident with the orientation of the patches in the perfect lattice. Therefore, the orientational partition function is given by:

$$Q_{Ein,or} = \left[\frac{1}{8\pi^2} \int \exp \left\{ -\beta(\Lambda_{E,a} \sin^2(\psi_{a,min}) + \Lambda_{E,b} \sin^2(\psi_{b,min})) \right\} \sin\theta d\theta d\phi d\chi \right]^N \quad (20)$$

In this case, the integral was evaluated numerically using the Monte Carlo integration method and using at least 10^9 points.

In all the cases, we have chosen that both the translational and orientational field have the same numeric value of the coupling parameter $\Lambda_E = \Lambda_{E,a} = \Lambda_{E,b}$. Note, however, that the coupling parameter of the translational field, Λ_E has units of energy over a squared length, whereas the orientational coupling parameters $\Lambda_{E,a}$ and $\Lambda_{E,b}$ have dimensions of energy.

Once the orientational field has been chosen, we can write the explicit form for the integral ΔA_2 . For example, for water:

$$\Delta A_2 = - \int_0^{\Lambda_E} \left\langle \sum_{i=2}^N (\mathbf{r}_i - \mathbf{r}_{io})^2 + \sum_{i=1}^N \left[\sin^2(\psi_{a,i}) + \left(\frac{\psi_{b,i}}{\pi} \right)^2 \right] \right\rangle_{N,V,T,\Lambda'} d\Lambda' \quad (21)$$

where the brackets with the subscript N, V, T, Λ' means an average over a simulation of a system where both an ideal Einstein field with coupling parameter Λ' (where $\Lambda' = \lambda\Lambda_E$) and the solid potential are present (i.e., the total potential is $U_{sol} + \Lambda' \sum_{i=2}^N (\mathbf{r}_i - \mathbf{r}_{io})^2 + \Lambda' \sum_{i=1}^N (\sin^2(\psi_{a,i}) + (\frac{\psi_{b,i}}{\pi})^2)$). For convenience, we will split this expression in two terms, one that accounts for the translational contribution ($\Delta A_{2,t}$) and other that accounts for the orientational contribution ($\Delta A_{2,or}$):

$$\Delta A_{2,t} = - \int_0^{\Lambda_E} \left\langle \sum_{i=2}^N (\mathbf{r}_i - \mathbf{r}_{io})^2 \right\rangle_{N,V,T,\Lambda'} d\Lambda' \quad (22)$$

$$\Delta A_{2,or} = - \int_0^{\Lambda_E} \left\langle \sum_{i=1}^N \left[\sin^2(\psi_{a,i}) + \left(\frac{\psi_{b,i}}{\pi} \right)^2 \right] \right\rangle_{N,V,T,\Lambda'} d\Lambda' \quad (23)$$

D. Finite size corrections

It is well known that the free energy of solids exhibits a strong size dependence.^{2,34,37,39,48} In a recent paper, we have made an attempt to propose some recipes to correct for this strong size dependence in a simple way. In what follows, we briefly review those FSC (a more detailed discussion was already given in Ref. 37).

The two first proposed FSC, namely, the Frenkel-Ladd FSC (FSC-FL) and the hard-spheres FSC (FSC-HS) consist of simply adding a term to the free energy of a system of N particles to obtain an approximation to the free energy in the thermodynamic limit:

$$\frac{A_{FSC-FL}}{Nk_B T}(N \rightarrow \infty) \simeq \frac{A_{solid}(N)}{Nk_B T} + \frac{2 \ln N}{N} \quad (24)$$

$$\frac{A_{FSC-HS}}{Nk_B T}(N \rightarrow \infty) \simeq \frac{A_{solid}(N)}{Nk_B T} + \frac{7}{N} \quad (25)$$

These are empiric corrections that have been shown to improve the results for the HS fcc solid. Also we have noted that the term $\frac{3}{2N} \ln N$ is approximately equal to the term $7/N$ except for very small values of N . Therefore, we decided to explore also the performance of this FSC:

$$\frac{A_{FSC-HS2}}{Nk_B T}(N \rightarrow \infty) \simeq \frac{A_{solid}(N)}{Nk_B T} + \frac{3 \ln N}{2 N} \quad (26)$$

In a second family of FSC which was designated as FSC-Asymptotic, the free energy in the thermodynamic limit is estimated by taking the limit when N tends to infinity in the analytical expression of the free energy of the ideal Einstein molecule (Eq. 9). Three different variants of the FSC-Asymptotic were proposed differing on whether a further approximation to the term ΔA_2 was also made. In the first variant ($A_{FSC-as1}$), no approximation was made to ΔA_2 :

$$\frac{A_{FSC-as1}}{Nk_B T}(N \rightarrow \infty) \simeq \frac{3}{2} \ln \left(\frac{\Lambda^2 \beta \Lambda_E}{\pi} \right) + \frac{A_{0,or}}{Nk_B T} + \frac{\Delta A_1(N, \Lambda_E)}{Nk_B T} + \frac{\Delta A_2(N, \Lambda_E)}{Nk_B T} \quad (27)$$

In a second variant, an approximation to ΔA_2 is made based on the assumption that all the $N - 1$ oscillators contribute by the same amount to the integral. This is a reasonable approximation for atomic solids (for a fcc HS solid with $N=108$ particles, we obtained that all the atoms except the first nearest neighbours contributed approximately by the same amount; the contribution of the nearest neighbours is about a 10% lower than the contribution of the remaining atoms). For molecular solids, it is important to notice that there are two contributions to ΔA_2 , one translational and one orientational. As pointed out before, the Einstein molecule only imposes the constraint on the position of particle 1, but not on its orientation. Therefore, assuming that all the molecules contribute by the same amount to the translational integral, ΔA_2 can be approximated by the following expression:

$$\frac{\Delta A_2}{Nk_B T} = \frac{\Delta A_{2,t}}{Nk_B T} + \frac{\Delta A_{2,or}}{Nk_B T} = \frac{N-1}{N} I_t + \frac{\Delta A_{2,or}}{Nk_B T} = \left(1 - \frac{1}{N} \right) I_t + \frac{\Delta A_{2,or}}{Nk_B T} \quad (28)$$

where $\Delta A_{2,t}$ and $\Delta A_{2,or}$ are given in Eq. 22 and 23, and I_t is the contribution to the translational integral of one single arbitrary particle (under the assumption that all the particles contribute by the same amount). We shall assume now that the orientational contribution is independent of the system size and that the asymptotic value of $\Delta A_{2,t}/Nk_B T$ is I_t . In the FSC-as2, ΔA_2 is approximated as:

$$\frac{\Delta A_2}{Nk_B T}(N \rightarrow \infty) \simeq I_t + \frac{\Delta A_{2,or}}{Nk_B T} \quad (29)$$

Therefore, the FSC-as2 for molecular solids must be slightly modified with respect to that obtained for atomic solids (compare with Eq. 35 of Ref. 37):

$$\begin{aligned} \frac{A_{FSC-as2}}{Nk_B T}(N \rightarrow \infty) \simeq & \frac{3}{2} \ln \left(\frac{\Lambda^2 \beta \Lambda_E}{\pi} \right) + \frac{A_{0,or}}{Nk_B T} + \frac{\Delta A_1(N, \Lambda_E)}{Nk_B T} \\ & + \frac{\Delta A_{2,or}(N, \Lambda_E)}{Nk_B T} + \frac{\Delta A_{2,t}(N, \Lambda_E)/(Nk_B T)}{(1 - 1/N)} \end{aligned} \quad (30)$$

Finally, the last variant is obtained as the mean value of the FSC-as1 and FSC-as2:

$$\begin{aligned} \frac{A_{FSC-as3}}{Nk_B T}(N \rightarrow \infty) \simeq & \frac{3}{2} \ln \left(\frac{\Lambda^2 \beta \Lambda_E}{\pi} \right) + \frac{A_{0,or}}{Nk_B T} + \frac{\Delta A_1(N, \Lambda_E)}{Nk_B T} + \frac{\Delta A_{2,or}(N, \Lambda_E)}{Nk_B T} + \\ & \frac{1}{2} \left(\frac{\Delta A_{2,t}(N, \Lambda_E)}{Nk_B T} + \frac{\Delta A_{2,t}(N, \Lambda_E)/(Nk_B T)}{(1 - 1/N)} \right) \end{aligned} \quad (31)$$

Notice that in these expressions ΔA_1 and ΔA_2 were obtained by the Einstein molecule approach.

III. RESULTS

A. The Einstein molecule approach

Before presenting the results of the free energy calculations with the Einstein molecule approach, we will show that fixing one molecule in a solid (in the absence of the Einstein field) does not affect the structural properties (due to the translational invariance). For that purpose, we computed the radial distribution function in a NVT simulation for an atomic system, the HS fcc solid, and the site-site radial distribution function for a molecular system, the hard-dumbbells CP1 solid. We will determine the structure both when one particle is fixed and when all the particles are allowed to move. For the HS fcc solid, we considered a simulation box with $N = 108$ particles, so that the possible existence of an inhomogeneity

would result in an appreciable change in the radial distribution function. As shown in Fig. 2 (a), the radial distribution function is identical regardless of whether one particle is fixed or not. As with regard to the hard-dumbbells CP1 solid, we considered a simulation box with only $N = 32$ particles. In this case the center of mass of molecule 1 was fixed but molecule 1 was allowed to rotate. Our results show that the site-site radial distribution function is again identical for a system where all the particles are allowed to move and for a system where the center of mass of one of the particles is fixed (see Fig. 2 (b)). Note that it is important that the dumbbell with fixed center of mass is allowed to rotate. If molecule 1 is frozen at a given orientation, the remaining molecules of the solid will not 'see' all the possible orientations of molecule 1. Therefore, all the possible orientations of the fixed molecule are not sampled and the fixed particle will introduce an inhomogeneity in the system. We checked that this is indeed true by computing also the site-site radial distribution function for a system where one particle is not allowed to translate and is not allowed to rotate. In this case, it is observed that the value of the site-site radial distribution function at contact is affected by the constraint on the orientation of the carrier molecule. In particular, we obtained that the value at contact is 5.072 when all the molecules are free to move, which is equal (within statistical error) to the value at contact when the position of molecule 1 is fixed but it is allowed to rotate, 5.070. However, when molecule 1 is not allowed to translate nor to rotate, the contact value of the radial distribution is somewhat lower (5.014), which means that the constraint on the orientation introduces an inhomogeneity in the solid.

The validity of the Einstein molecule approach for molecular solids was checked by comparing the free energies of different molecular solids with those obtained using the Frenkel-Ladd Einstein crystal method (as implemented by Polson *et al.*³⁹). At this stage, as the purpose was to show that both methods lead to exactly the same results, we performed unusually long simulations in order to reduce the statistical error. In what follows, we describe the simulation details for each model.

For the HD CP1 solid, we calculated the free energy for a system with $N = 144$ ($6 \times 6 \times 4$ unit cells) at a number density $\rho^* = \rho \sigma_{HS}^3 = 0.590$, where σ_{HS} is the diameter of each one of the hard-spheres of a hard-dumbbell. As the solid is not cubic, we first performed a Parrinello-Rahman^{69,70} NpT MC simulation consisting of 5×10^5 MC cycles for equilibration plus another 5×10^5 MC cycles for taking averages (a MC cycle is defined as N attempts to translate or rotate a particle plus one attempt to change the the matrix that defines

the simulation box). In agreement with previous calculations, the Parrinello-Rahman NpT simulations show that the ratio between the two edges of the unit cell (c/a) is slightly different from that at close-packing. Besides the changes in the shape of the simulation box it is observed that the orientation of the hard-dumbbells is also different from that at close-packing. They change from $\theta = 35.26^\circ$ to $\theta \approx 32^\circ$ and from $\phi = 30^\circ$ to $\phi \approx 31^\circ$. This has already been noted by Vega *et al.*⁹ Once we have obtained the equilibrium configuration at $\rho^* = 0.590$, the free energy was calculated by using 16 points to evaluate the integral ΔA_2 by the Gauss-Legendre quadrature formula. At each point, the integrand of ΔA_2 was evaluated by performing a NVT MC simulation consisting of 2×10^5 MC cycles for equilibration and 2×10^6 MC cycles for taking averages at each value of the coupling parameter. The term ΔA_1 was calculated in a simulation consisting of 2×10^5 MC cycles for equilibration and 5×10^5 MC cycles for taking averages. The maximum value of the coupling parameter used for the free energy calculations was $\Lambda_E/(k_B T/\sigma_{HS}^2) = 4000$.

For the patchy model we considered two system sizes $N = 125$ and $N = 216$. In both cases, the free energy was computed at the same thermodynamic state, $T^* = T/(\varepsilon_{LJ}/k_B) = 0.2$ and $\rho^* = \rho\sigma_{LJ}^3 = 0.763$, where ε_{LJ} and σ_{LJ} are the parameters of the LJ potential. The free energy was evaluated by using 20 points to compute ΔA_2 , and at each of those points we performed a simulation using 2×10^5 MC cycles for equilibration and 1×10^6 cycles for taking averages. A maximum value of $\Lambda_E/(k_B T/\sigma_{LJ}^2) = \Lambda_{E,a}/(k_B T) = \Lambda_{E,b}/(k_B T) = 20000$ was used.

Finally, for ices XIII and XIV (two recently discovered solid phases of water that exhibit both oxygen and proton ordering), we computed the free energy at $p = 1$ bar and $T = 80K$. The simulation box contained $3 \times 3 \times 2$ unit cells (504 molecules) in the case of ice XIII and $3 \times 3 \times 5$ unit cells (540 molecules) for ice XIV. As mentioned before, neither of these solid phases has cubic symmetry. Ice XIII has a monoclinic unit cell and ice XIV has an orthorhombic unit cell. Therefore, previously to the computation of the free energy, the solid structure was relaxed to the equilibrium. For ice XIII, we obtained that, at $p = 1$ bar and $T = 80K$, the equilibrium simulation box corresponds to $a = 20.39 \text{ \AA}$, $b = 22.09 \text{ \AA}$ and $c = 28.15 \text{ \AA}$, and $\beta = 109,6^\circ$ (α and γ are equal to 90°). As ice XIV has orthorhombic symmetry, only the length of the edges of the box were allowed to fluctuate in the simulations, while the angles were kept fixed. In this case, it was obtained that, at this thermodynamic state, the length of the edges of the simulation box at equilibrium are

$a = 24.45 \text{ \AA}$, $b = 25.17 \text{ \AA}$ and $c = 19.72 \text{ \AA}$. Once that the equilibrium shape of the simulation box was obtained, the positions and orientations of the molecules (i.e, the positions of the oxygens and hydrogens) in the reference structure were taken from the crystallographic data provided by Salzmann *et al.*⁶¹ The NpT simulations consisted of 5×10^4 MC cycles for equilibration and 1.5×10^5 cycles for taking averages. The free energy was computed using a maximum value of $\Lambda_E/(k_B T/\text{\AA}^2) = \Lambda_{E,a}/(k_B T) = \Lambda_{E,b}/(k_B T) = 25000$. 16 points were used to evaluate the term ΔA_2 and, at each of these points, a simulation consisting of 5×10^5 MC cycles (3×10^4 cycles for equilibration) was carried out, while the term ΔA_1 was obtained from a simulation consisting of 1×10^6 MC cycles (2×10^5 for equilibration).

The results of the free energies for these systems, as calculated using the Einstein crystal method and the Einstein molecule approach are shown in Tables I and II. In addition to the total free energy, the value of the different terms that contribute to the free energy in both methods are also shown. It can be seen that both methods give the same value of the free energy within the statistical uncertainty. Although the contribution of the different terms that contribute to the free energy is not the same when the center of mass is fixed or when molecule 1 is fixed, their sum is invariant. It is interesting to note that the difference between $\Delta A_2^*/Nk_B T$ and $\Delta A_2/Nk_B T$ is about $\frac{3}{2N} \ln N$ (see discussion in Ref. 38). Therefore, our results show that, indeed, the Einstein molecule approach is a valid route to compute the free energy of molecular solids.

B. Free energy of ices XIII and XIV.

As this is the first time that the free energies of ices XIII and XIV are given, we decided to perform more extensive calculations in this case. The effect of the shape of the simulation box on the free energy was also studied. Moreover, as mentioned before, it is not obvious what orientation of the water molecules should be chosen in the reference structure. For that reason, we decided to explore some of the possible orientations to see whether this choice affects the results of the free energy calculations. The results presented in this section have been obtained from shorter simulations than those of the previous section. Typically each simulation consisted of 2×10^5 MC cycles (4×10^4 for equilibration). This is usually enough to obtain a reasonable accuracy.

First we calculated the free energy of both phases using the Einstein molecule ap-

proach in three different thermodynamic states, namely, $p=1\text{bar}$ and $T=80\text{K}$, $p=1\text{bar}$ and $T=250\text{K}$ and $p=5000\text{bar}$ and $T=80\text{K}$, so that there are two points along one isobar and two points along one isotherm. The values of the free energies at those thermodynamic states are shown in Table III. These data will serve us to check that our calculations are thermodynamically consistent, i.e., that the results of the free energy calculations are the same as those obtained by thermodynamic integration of the equation of state. For ice XIII, through free energy calculations, we obtained $A_1(80\text{K}, 1\text{bar}) = -77.51(4)Nk_B T$, $A_2(80\text{K}, 5000\text{bar}) = -77.39(4)Nk_B T$ and $A_3(250\text{K}, 1\text{bar}) = -18.51(4)Nk_B T$. Starting from A_1 and performing thermodynamic integration along this isotherm we obtained that $A_2(80\text{K}, 5000\text{bar}) = -77.40(6)Nk_B T$. The integration along the isobar starting from A_1 yields $A_3(250\text{K}, 1\text{bar}) = -18.46(6)Nk_B T$. Both estimations are in agreement with the results obtained by means of free energy calculations. A good agreement was also obtained for ice XIV. In this case, the free energy calculations provide $A_1(80\text{K}, 1\text{bar}) = -77.82(4)Nk_B T$, $A_2(80\text{K}, 5000\text{bar}) = -77.73(4)Nk_B T$, and $A_3(250\text{K}, 1\text{bar}) = -18.45(4)Nk_B T$. Starting from A_1 and integrating along the isotherm 80K , we obtained that $A_2(80\text{K}, 5000\text{bar}) = -77.74(6)Nk_B T$, and integrating along the isobar 1bar , it is obtained that $A_3(250\text{K}, 1\text{bar}) = -18.52(6)Nk_B T$, again in good agreement with the results of free energy calculations.

Once we have confidence on the reliability of our calculations, we studied the effect of the shape of the simulation box on the free energy. For that purpose, for ice XIV, the free energy was also computed for a simulation box that has been deformed from the equilibrium shape at $T=80\text{K}$ and $p=1\text{bar}$. The length of the edges at equilibrium $L_{x,0}$, $L_{y,0}$ and $L_{z,0}$, were deformed to $L'_x = L_{x,0} \times \alpha$, $L'_y = L_{y,0} \times \alpha$, and $L'_z = L_{z,0}/\alpha^2$, so that the density remains invariant under this change of the simulation box. Our results show that the free energy increases when the shape of the simulation box does not correspond to that at equilibrium. In particular, when a deformation defined by $\alpha = 0.96$ is applied, the free energy increases from its value at equilibrium $A_{sol}/(Nk_B T) = -77.82(4)$ to $A_{sol}/(Nk_B T) = -77.00(4)$. An increase is also found when the edges are scaled with $\alpha = 1.04$, for which it was found that $A_{sol}/(Nk_B T) = -77.10(4)$. This is the expected result, as the equilibrium structure corresponds to a minimum of free energy, and any perturbation will result in an increase of the free energy. These results evidence the importance of obtaining the equilibrium structure previously to the computation of the free energy. Otherwise, we would be overestimating the value of the free energy.

As mentioned before, the positions of the oxygens and hydrogens (i.e., the position and orientation of the water molecules) in the reference structure to be used for the Einstein field were taken from the experimental values (for ices XIII and XIV both the oxygen and hydrogens are ordered). However, the experimental equilibrium positions and orientations of the molecules will not be exactly equal to those of the potential model used in the simulations. Moreover, it is possible that one would want to study some solid for which there are no experimental data available. This does not pose a problem, because, in principle, the free energy should not depend on the precise location of the external field provided that the field reflects the structure of the system. However, we wanted to check that this was indeed true and we computed the free energy using another reference structure. In particular, we now used a reference structure in which the water molecules are oriented as to minimise the potential energy. This structure was obtained by simulated annealing. Starting from a configuration in which the simulation box corresponds to the equilibrium (as obtained from the NpT simulation) and where the water molecules have the same positions and orientation as those found in experiments, we performed a quenching from 80K to 1K, using 6 intermediate temperatures, and keeping the shape of the simulation box constant along the whole simulation. At each one of the temperatures, the system was allowed to evolve during 2×10^4 MC cycles. To avoid translations of the system as a whole, we fixed the reference point (but not the orientation) of molecule 1 in the annealing. The structure obtained from the annealing should be close to the minimum in the potential energy (the minimum energy structure would be obtained at 0K, at 1K the structure is likely to be not yet at the minimum⁷¹). Using the structures obtained from simulated annealing, we calculated again the free energies of ices XIII and XIV (see Table III). It can be seen that the free energy is independent of the reference structure. As expected, the terms ΔA_1 and ΔA_2 take different values depending on which reference structure has been chosen. However, their sum is independent of the reference structure. The term ΔA_1 is close to the lattice energy and, therefore, it is obvious that its value will depend on the reference structure. On the other hand, ΔA_2 is the integral from the real solid to the Einstein molecule with intermolecular interactions. In this case, the fact of changing the reference structure means that the integral is performed from a new starting point, which results on a different value of the integral ΔA_2 . However, our results show that the changes in ΔA_1 and ΔA_2 cancel out and, therefore, the same value of the free energy is obtained regardless of which

reference structure has been used. Finally we also evaluated the free energy for a reference structure in which the atoms are located at their average positions and orientations at that thermodynamic state (these were obtained by averaging over 500 snapshots and readjusting the positions of the hydrogens to obtain the bond and angle distances of the TIP4P/2005 model for each molecule), and again the same value of the free energy (within statistical error) is obtained. Obviously, it is desirable that the reference structure is close to the equilibrium structure, otherwise larger values of the coupling parameter would be needed and this will result in a higher statistical error in the evaluation of ΔA_2 .

Taking into account all these considerations, the procedure to compute the free energy is schematically described in Fig. 3. It is important that, previously to the computation of the free energy, an appropriate reference structure is obtained.

Before leaving this Section and because this is the first time that the free energy of ices XIII and XIV has been computed, we would like to briefly discuss the relative stability of these two ice polymorphs. For that purpose, we computed the chemical potential [$\beta\mu = (\beta A/N) + (P/\rho k_B T)$] along the isobars $p=1\text{bar}$ and $p=5000\text{bar}$ by thermodynamic integration (see Fig. 4). It can be seen that, at $p=5000\text{bar}$ ice XIV is more stable than ice XIII at all temperatures, i.e., from low temperatures up to melting temperatures. On the contrary, at $p=1\text{bar}$, ice XIV is slightly more stable than ice XIII at low temperatures, but at temperatures close to melting ice XIII seems to be slightly more stable than ice XIV. The phase transition seems to occur around $T \approx 187\text{K}$. In any case, it is important to note that ice I_h is the most stable phase at $p = 1 \text{ bar}$ for the TIP4P/2005 model.⁵⁴

C. Size dependence of the free energy of molecular solids

Finally we also studied the size dependence of the free energy of molecular solids by analysing the size behaviour of three different solid structures (sc, bcc, and fcc) for the octahedral patchy model. The free energies of those solid structures as obtained in this work using the Einstein molecule approach for several values of N are given in Table IV. Results for the LJ fcc solid at $T^* = 0.2$ and $\rho^* = 1.28$ are also given in Table V. In these calculations, the LJ potential was truncated at a cutoff distance of 2.7σ and long range corrections were used (obtained assuming $g(r) = 1$ beyond the cutoff). Our results show that for all the studied solid structures the free energy exhibits a strong size dependence,

as found in previous studies.^{2,34,37,39,48} It is interesting to note that the slope of the plot $A(N)/Nk_B T$ versus $1/N$ is different depending on the solid structure, even for the same model potential. For the patchy model, we obtained that the slope is about -14 for the sc structure, about -8 for the bcc and about -12 for the fcc. This means that, in order to accurately calculate the phase diagram of a given substance, a study of the system size dependence must be performed for each considered solid structure, which implies a large number of simulations. Therefore it would be useful to have a simple recipe to correct for the system size dependence as this could save a large amount of computational time.

The performance of the FSC was studied for all the considered solid structures of the octahedral anisotropic model. In Tables IV and V, all the contributions to the free energy are explicitly given, as this will allow us to identify the terms that exhibit a stronger dependence with the system size. The free energy obtained by applying the proposed FSC to the free energy at a given N for all the considered solid structures of the octahedral patchy model are given in Table VI and in Figure 5. Results of applying the FSC to the calculated free energies of the fcc LJ solid are also given in Table VI. It can be seen that all the proposed recipes for finite size corrections give a value of the free energy closer to the thermodynamic limit than the estimate obtained from the value of the free energy for a certain N . The FSC-HS, which was based on the slope of the free energy as a function of $1/N$ for HS, obviously works better when the slope is similar to the slope of HS (around -7). The same is true for the FSC-HS2. Therefore, at a given size, the prediction of the value of the free energy in the thermodynamic limit for the sc and fcc structures for the patchy model, whose slopes were -14 and -12, respectively, is not very accurate. The performance of the FSC-FL is also not satisfactory. Although it also seems to give quite good results in some cases (e.g., for the bcc solid in the patchy model), there are other solids for which they correct only partially for the system size dependence. Finally, the FSC-Asymptotic in its three variants seem to give quite accurate results for all the cases studied. This can be understood by looking at the size dependence of the terms that contribute to the free energy (see Tables IV and V). It can be observed that the terms ΔA_1 and the orientational contribution to ΔA_2 ($\Delta A_{2,or}$) are almost independent of the system size. All the size dependence comes from the free energy of the reference system (as given by Eq. 9) and, to a much lesser extent, from the translational contribution to the integral ΔA_2 ($\Delta A_{2,t}$). Therefore, by simply taking the limit when $N \rightarrow \infty$ in this analytical expression (Eq. 9), the free energy at a given N can

be substantially corrected.

We also calculated the deviation from the correct value (i.e., the free energy in the thermodynamic limit) for all the proposed FSC (see Table VII). Data for the HS fcc solid at three different thermodynamic states taken from a previous work³⁷ are also included in Table VII. The deviation from the correct value ($d = \frac{A_{sol}(N)}{Nk_B T} - \frac{A_{sol}(N=\infty)}{Nk_B T}$) was computed for the lowest system size studied in each case. The mean deviation of each FSC computed as $\bar{d} = (\sum_{i=1}^n |d|/n) \times 1000$ is also given. It can be seen that both the FSC-as1 and the FSC-as3 exhibit the best performance, obtaining a mean deviation from the correct value of 7 or 8 (in $10^{-3}Nk_B T$ units). The deviation of the rest of the FSC is not as good, but still the mean deviation is typically around 14, which is substantially lower than the mean deviation obtained from the true value of the free energy at small values of N (around 55).

IV. CONCLUSIONS

In this paper, we have extended the Einstein molecule approach to the computation of the free energy of molecular solids. The method has been tested using a variety of model potentials, which include hard-dumbbells, the TIP4P/2005 water model and a simple anisotropic model consisting of a spherical repulsive core with some attractive sites. Our results show that both the Einstein crystal method of Frenkel and Ladd (as corrected by Polson *et al.*³⁹) and the Einstein molecule approach of Vega and Noya give the same results of the free energy within statistical accuracy.

Once the Einstein molecule approach was tested, this method was used to compute the free energies of ices XIII and XIV for first time. The free energy was computed at three different thermodynamic states, which allowed us to test our free energy calculations by performing thermodynamic consistency checks. In addition, we have stressed the importance of using the equilibrium shape of the simulation box in the computation of the free energy. Our results show that any deformation from this equilibrium structure invariably leads to an increase of the free energy. This is the expected behaviour, as the equilibrium structure is that that minimises the free energy. Any deformation introduces stress in the system that leads to an increase of the free energy. Therefore, for solids with non-cubic symmetry, it is important to perform a Parrinello-Rahman NpT simulation to obtain the equilibrium shape of the simulation box previously to the computation of the free energy.

Moreover, we studied the effect that the choice of the reference Einstein field has on the calculation of free energies. In complex solids, such as, for example, ices XIII and XIV, there is not an obvious choice of how the water molecules should be oriented in the reference structure, as both solids exhibit a complex unit cell with a large number of water molecules and in which not all the molecules exhibit the same orientation. We have performed calculations of the free energy of both solid phases using a reference structure where the positions and orientations of the molecules were taken from experimental data and using a reference structure that has been obtained by simulated annealing, i.e., using a reference structure that minimises the potential energy (for the equilibrium shape of the simulation box). Our results show that, even though the two choices lead to different values of ΔA_1 and ΔA_2 , the addition of both terms is independent of the choice of the reference structure. This is the expected result, because we are computing the free energy of the same solid, but using a different reference system (i.e., the position and orientation of the field are slightly different). Obviously it is desirable to use a reference structure that is close to the minimum, otherwise larger values of the coupling parameter will be needed and this will result in a larger error in the evaluation of ΔA_2 . This is an important result, because, in many cases, one will be interested in real solids with complex structures and the choice of a reference structure will be a subtle issue. However, our results show that it is not necessary to obtain the structure that minimises the potential energy, as far as the reference structure is not too far from this minimum.

Finally, we have also studied the size dependence of the free energy for a simple anisotropic model. Our results show that all the studied solid phases, namely, sc, bcc, and fcc, exhibit a strong size dependence, although the slope of the plot of A versus $1/N$ is different for each solid phase. In a previous work we also found that the free energy of the fcc HS solid depends slightly on the density.³⁷ This means that there is a complex dependence of the free energy with the system size, which depends not only on the model potential, but also on the thermodynamic state and on the solid structure. This result seems to suggest that it might be difficult to obtain a simple recipe that would allow us to obtain the free energy in the thermodynamic limit from the calculated value at a finite size N . In any case, we tested all the previously proposed FSC and we found that the asymptotic FSC-as1 and FSC-as3 manage to give quite accurate estimates of the free energy in the thermodynamic limit for all the solids studied so far.

Acknowledgments

This work was funded by grants FIS2007-66079-C02-01 of Dirección General de Investigación and S-0505/ESP/0229 from the Comunidad Autónoma de Madrid. E.G.N. wishes to thank the Ministerio de Educación y Ciencia and the Universidad Complutense de Madrid for a Juan de la Cierva fellowship. M. M. Conde would like to thank Universidad Complutense by the award of a PhD grant.

Appendix

We will show that the free energy of the ideal Einstein molecule (Eq. 9) can be obtained as a particular case of the ideal Einstein crystal with fixed center of mass. In the ideal Einstein molecule the free energy is given by:

$$A_{sol} = A_{Ein-mol-id} + \Delta A_1 + \Delta A_2 = A_0 + \Delta A_1 + \Delta A_2 \quad (32)$$

The precise expression for A_0 is just that of $A_{Ein-mol-id}$ (see Eq. 9).

In the Einstein crystal method the free energy is computed following the integration path shown in Fig. 1 , so that the free energy can be computed as:

$$A_{sol} = (A_{Ein-id}^{CM} + \Delta A_3^*) + \Delta A_1^* + \Delta A_2^* = A_0^* + \Delta A_1^* + \Delta A_2^* \quad (33)$$

$$A_0^* = A_{Ein-id}^{CM} + \Delta A_3^* \quad (34)$$

In this appendix we will show that for a particular choice of the mass of the particles the Einstein crystal expression reduces to that of the Einstein molecule expression. The term A_{Ein-id}^{CM} is given by :

$$A_{Ein-id}^{CM} = -kT \ln(Q_{Ein,t}^{CM}) - kT \ln(Q_{Ein,or}) \quad (35)$$

where $Q_{Ein,t}^{CM}$ is given by (see Eq. 97 of Ref. 38) :

$$Q_{Ein,t}^{CM} = P^{CM}(m_1, \dots, m_N) \left(\frac{\pi}{\beta \Lambda_E} \right)^{3(N-1)/2} \left(\sum_{i=1}^N \mu_i^2 \right)^{-3/2}, \quad (36)$$

and $P^{CM}(m_1, \dots, m_N)$ is the contribution of the momenta integral in a system with fixed center of mass, where the dependence of $P^{CM}(m_1, \dots, m_N)$ on the masses is written explicitly.

The term ΔA_3^* is given by :

$$\Delta A_3^* = k_B T [\ln(P^{CM}(m_1, \dots, m_N)/P) - \ln(V/N)] \quad (37)$$

where $P = 1/(\prod_{i=1}^N \Lambda_i^3)$ is the contribution to the space of momenta for an unconstrained solid.

Putting together all terms contributing to A_0^* one obtains:

$$A_0^* = -k_B T \ln \left(\frac{1}{\prod_{i=1}^N \Lambda_i^3} \frac{V}{N} \left(\frac{\pi}{\beta \Lambda_E} \right)^{3(N-1)/2} \left(\sum_{i=1}^N \mu_i^2 \right)^{-3/2} \right) - k_B T \ln(Q_{Ein,or}) \quad (38)$$

Let us now compute $Q_{Ein,t}^{CM}$ for the case where all particles of the system have the same mass, $m_2 = m_3 = \dots = m_N$, but the mass of molecule 1 becomes infinitely large compared to that of the rest of the particles of the system (this is the choice of Vega and Noya³⁷). In this case $\mu_1 = 1$ and all $\mu_2 = \mu_3 = \dots = \mu_N = 0$ (where $\mu_i = m_i / \sum_{i=1}^N m_i$). Obviously under these circumstances fixing the center of mass is equivalent to fixing the position of molecule 1 and, therefore, $\Delta A_1^* = \Delta A_1$ and $\Delta A_2^* = \Delta A_2$. Let us see if for this particular choice we also obtain that $A_0^* = A_0$ which will complete the proof. Substituting the reduced masses $\mu_1 = 1$ and all $\mu_2 = \mu_3 = \dots = \mu_N = 0$ in the expression of A_0^* , and after some reordering of the terms, one obtains:

$$A_0^* = k_B T \ln \left(\frac{N \Lambda^3}{V} \right) + k_B T \ln \left(\frac{\Lambda^2 \beta \Lambda_E}{\pi} \right)^{3(N-1)/2} - k_B T \ln(Q_{Ein,or}) + k_B T \ln \left(\frac{\Lambda_1^3}{\Lambda^3} \right) \quad (39)$$

which is exactly equal to the expression of A_0 in the Einstein molecule method (Eq. 9), except for the trivial term $k_B T \ln \left(\frac{\Lambda_1^3}{\Lambda^3} \right)$, which obviously will also appear in the fluid phase and will not affect the phase equilibria. Thus we have proved that the Einstein molecule method can be obtained as a limit case of the Einstein crystal method.

We have seen that the precise value of P^{CM} is irrelevant to compute the free energy (i.e., it does not appear in the expression of A^* as given by Eq. 38). Nevertheless, for completeness, we will compute its value for the two cases we are considering. We will start from the general expression of $P^{CM}(m_1, \dots, m_N)$:

$$P^{CM}(m_1, \dots, m_N) = \frac{1}{h^{3(N-1)}} \int \exp \left[-\beta \sum_{i=1}^N \frac{\mathbf{p}_i^2}{2m_i} \right] \delta \left(\sum_{i=1}^N \mathbf{p}_i \right) d\mathbf{p}_1 \dots d\mathbf{p}_N \quad (40)$$

In the particular case that all particles of the system have the same mass (this is the choice made by Polson et al.) then for all particles $m_i = m$ and $\mu_i = 1/N$ and then:

$$P^{CM}(m, \dots, m) = \frac{1}{\Lambda^{3(N-1)}} N^{-3/2} \quad (41)$$

and

$$Q_{Ein,t}^{CM} = \left(\frac{1}{\Lambda} \right)^{3(N-1)} \left(\frac{\pi}{\beta \Lambda_E} \right)^{3(N-1)/2} \quad (42)$$

See the derivation of this equation in Ref. 38 (Eq. 101).

Let us now compute P^{CM} for the case where all particles of the system have the same mass, $m_2 = m_3 = \dots = m_N$, but the mass of molecule 1 becomes infinitely large compared to that of the rest of the particles of the system (this is the choice of Vega and Noya). In this case $\mu_1 = 1$ and all $\mu_2 = \mu_3 = \dots = \mu_N = 0$.

For this choice of masses:

$$P^{CM} = \frac{1}{h^{3(N-1)}} \int \exp \left[-\beta \sum_{i=1}^N \frac{\mathbf{p}_i^2}{2m_i} \right] \delta(\mathbf{p}_1) d\mathbf{p}_1 \dots d\mathbf{p}_N \quad (43)$$

where $\sum_{i=1}^N \mathbf{p}_i = 0$ was simplified to $\mathbf{p}_1 = 0$ when the mass of molecule 1 becomes infinitely large.

It is straightforward to integrate this expression to obtain:

$$P^{CM} = \frac{1}{h^{3(N-1)}} \left(\frac{2m\pi}{\beta} \right)^{3(N-1)/2} = \left(\frac{1}{\Lambda} \right)^{3(N-1)} \quad (44)$$

Therefore, the translational contribution to the partition function is:

$$Q_{Ein,t}^{CM} = \left(\frac{1}{\Lambda} \right)^{3(N-1)} \left(\frac{\pi}{\beta\Lambda_E} \right)^{3(N-1)/2}, \quad (45)$$

which is identical to the expression obtained for the case where all particles have the same mass (Eq. 42). Therefore the expression for A_{Ein-id}^{CM} is the same when all particles have the same mass or for the case where all have the same mass but particle 1 which becomes infinitely heavy.

The partition function of an unconstrained Einstein crystal is given by:

$$Q_{Ein} = \left(\frac{1}{\Lambda} \right)^{3N} \left(\frac{\pi}{\beta\Lambda_E} \right)^{3N/2} \quad (46)$$

so that constraining the center of mass in the Einstein crystal amounts to reducing the number of degrees of freedom by 3. Notice that this is not the same as ΔA_3^* as given by Eq. 37. The reason is that Eq. 37 gives the change in free energy for fixing the center of mass in a system with translational invariance (i.e., the energy of the system is invariant to a translation $\mathbf{\Delta}$ of all the particles), and such invariance has been used in the derivation leading to the term $-\ln(V/N)$. Notice that the Einstein crystal does not have translational invariance (the energy changes when all the particles are translated by $\mathbf{\Delta}$ since the lattice does not move), so that ΔA_3^* cannot be used to get the free energy change for fixing the center of mass in this case.

-
- ¹ W. G. Hoover and F. H. Ree, *J. Chem. Phys.* **49**, 3609 (1968).
 - ² D. Frenkel and A. J. C. Ladd, *J. Chem. Phys.* **81**, 3188 (1984).
 - ³ D. Frenkel and B. M. Mulder, *Molec. Phys.* **55**, 1171 (1985).
 - ⁴ C. Vega and P. A. Monson, *J. Chem. Phys.* **109**, 9938 (1998).
 - ⁵ M. J. Vlot, J. Huinink, and J. P. van der Eerden, *J. Chem. Phys.* **110**, 55 (1999).
 - ⁶ G. Grochola, *J. Chem. Phys.* **120**, 2122 (2004).
 - ⁷ D. M. Eike, J. F. Brennecke, and E. J. Maginn, *J. Chem. Phys.* **122**, 014115 (2005).
 - ⁸ M. B. Sweatman, *Phys. Rev. E* **72**, 016711 (2005).
 - ⁹ C. Vega, E. P. A. Paras, and P. A. Monson, *J. Chem. Phys.* **96**, 9060 (1992).
 - ¹⁰ A. Stroobants, H. N. W. Lekkerkerker, and D. Frenkel, *Phys. Rev. Lett.* **57**, 1452 (1986).
 - ¹¹ J. A. C. Veerman and D. Frenkel, *Phys. Rev. A* **41**, 3237 (1990).
 - ¹² C. Vega, E. P. A. Paras, and P. A. Monson, *J. Chem. Phys.* **97**, 8543 (1992).
 - ¹³ A. P. Malanoski and P. A. Monson, *J. Chem. Phys.* **107**, 6899 (1997).
 - ¹⁴ J. M. Polson and D. Frenkel, *J. Chem. Phys.* **109**, 318 (1998).
 - ¹⁵ A. P. Malanoski and P. A. Monson, *J. Chem. Phys.* **110**, 664 (1999).
 - ¹⁶ F. Bresme, C. Vega, and J. L. F. Abascal, *Phys. Rev. Lett.* **85**, 3217 (2000).
 - ¹⁷ G. T. Gao, X. C. Zeng, and H. Tanaka, *J. Chem. Phys.* **112**, 8534 (2000).
 - ¹⁸ J. W. Schroer and P. A. Monson, *J. Chem. Phys.* **112**, 8950 (2000).
 - ¹⁹ J. W. Schroer and P. A. Monson, *J. Chem. Phys.* **114**, 4124 (2001).
 - ²⁰ E. de Miguel and C. Vega, *J. Chem. Phys.* **117**, 6313 (2002).
 - ²¹ F. J. Blas, E. Sanz, C. Vega, and A. Galindo, *J. Chem. Phys.* **119**, 10958 (2003).
 - ²² J. Anwar, D. Frenkel, and M. G. Noro, *J. Chem. Phys.* **118**, 728 (2003).
 - ²³ C. Vega, J. L. F. Abascal, C. McBride, and F. Bresme, *J. Chem. Phys.* **119**, 964 (2003).
 - ²⁴ A. P. Hynninen and M. Dijkstra, *Phys. Rev. E* **68**, 021407 (2003).
 - ²⁵ A. P. Hynninen and M. Dijkstra, *J. Phys. Cond. Mat.* **15**, S3557 (2003).
 - ²⁶ Y. Koyama, H. Tanaka, G. Gao, and X. C. Zeng, *J. Chem. Phys.* **121**, 7926 (2004).
 - ²⁷ E. Sanz, C. Vega, J. L. F. Abascal, and L. G. MacDowell, *Phys. Rev. Lett.* **92**, 255701 (2004).
 - ²⁸ E. Sanz, C. Vega, J. L. F. Abascal, and L. G. MacDowell, *J. Chem. Phys.* **121**, 1165 (2004).
 - ²⁹ I. Saika-Voivod, F. Sciortino, T. Grande, and P. H. Poole, *Phys. Rev. E* **70**, 061507 (2004).

- ³⁰ L. M. Ghiringhelli, J. H. Los, E. J. Meijer, A. Fasolino, and D. Frenkel, *Phys. Rev. Lett.* **94**, 145701 (2005).
- ³¹ A. Fortini and M. Dijkstra, *J. Phys. Cond. Mat.* **18**, L371 (2006).
- ³² A. P. Hynninen, M. E. Leunissen, A. van Blaaderen, and M. Dijkstra, *Phys. Rev. Lett.* **96**, 018303 (2006).
- ³³ J. B. Caballero, E. G. Noya, and C. Vega, *J. Chem. Phys.* **127**, 244910 (2007).
- ³⁴ E. de Miguel, R. G. Marguta, and E. M. del Rio, *J. Chem. Phys.* **127**, 154512 (2007).
- ³⁵ N. G. Almarza, *J. Chem. Phys.* **126**, 211103 (2007).
- ³⁶ J. Chang and S. I. Sandler, *J. Chem. Phys.* **118**, 8390 (2003).
- ³⁷ C. Vega and E. G. Noya, *J. Chem. Phys.* **127**, 154113 (2007).
- ³⁸ C. Vega, E. Sanz, J. L. F. Abascal, and E. G. Noya, *J. Phys. Cond. Mat.* **20**, 153101 (2008).
- ³⁹ J. M. Polson, E. Trizac, S. Pronk, and D. Frenkel, *J. Chem. Phys.* **112**, 5339 (2000).
- ⁴⁰ P. Bolhuis and D. Frenkel, *J. Chem. Phys.* **106**, 666 (1997).
- ⁴¹ E. G. Noya, C. Vega, and E. de Miguel, *J. Chem. Phys.* **128**, 154507 (2008).
- ⁴² L. A. Báez and P. Clancy, *Molec. Phys.* **86**, 385 (1995).
- ⁴³ N. B. Wilding and A. D. Bruce, *Phys. Rev. Lett.* **85**, 5138 (2000).
- ⁴⁴ N. B. Wilding, *Comp. Phys. Comm.* **146**, 99 (2002).
- ⁴⁵ A. D. Bruce, N. B. Wilding, and G. J. Ackland, *Phys. Rev. Lett.* **79**, 3002 (1997).
- ⁴⁶ A. D. Bruce, A. N. Jackson, G. J. Ackland, and N. B. Wilding, *Phys. Rev. E* **61**, 906 (2000).
- ⁴⁷ A. D. Bruce and N. B. Wilding, *Adv. Chem. Phys.* **127**, 1 (2003).
- ⁴⁸ M. A. Barroso and A. L. Ferreira, *J. Chem. Phys.* **116**, 7145 (2002).
- ⁴⁹ M. Marechal and M. Dijkstra, *Phys. Rev. E* **77**, 061405 (2008).
- ⁵⁰ C. Vega and L. G. MacDowell, *J. Chem. Phys.* **114**, 10411 (2001).
- ⁵¹ C. Vega, L. G. MacDowell, C. McBride, F. J. Blas, A. Galindo, and E. Sanz, *J. Molec. Liq.* **113**, 37 (2004).
- ⁵² C. Vega and P. A. Monson, *J. Chem. Phys.* **107**, 2696 (1997).
- ⁵³ K. W. Wojciechowski, D. Frenkel, and A. C. Branka, *Phys. Rev. Lett.* **66**, 3168 (1991).
- ⁵⁴ J. L. F. Abascal and C. Vega, *J. Chem. Phys.* **123**, 234505 (2005).
- ⁵⁵ W. L. Jorgensen, J. Chandrasekhar, J. D. Madura, R. W. Impey, and M. L. Klein, *J. Chem. Phys.* **79**, 926 (1983).
- ⁵⁶ C. Vega, C. McBride, E. Sanz, and J. L. Abascal, *Phys. Chem. Chem. Phys.* **7**, 1450 (2005).

- ⁵⁷ R. G. Fernandez, J. L. F. Abascal, and C. Vega, *J. Chem. Phys.* **124**, 144506 (2006).
- ⁵⁸ J. L. F. Abascal, E. Sanz, R. G. Fernández, and C. Vega, *J. Chem. Phys.* **122**, 234511 (2005).
- ⁵⁹ H. W. Horn, W. C. Swope, J. W. Pitera, J. D. Madura, T. J. Dick, G. L. Hura, and T. Head-Gordon, *J. Chem. Phys.* **120**, 9665 (2004).
- ⁶⁰ E. G. Noya, C. Menduina, J. L. Aragonés, and C. Vega, *J. Phys. Chem. C* **111**, 15877 (2007).
- ⁶¹ C. G. Salzmann, P. G. Radaelli, A. Hallbrucker, E. Mayer, and J. L. Finney, *Science* **311**, 1758 (2006).
- ⁶² M. Martin-Conde, L. G. MacDowell, and C. Vega, *J. Chem. Phys.* **125**, 116101 (2006).
- ⁶³ M. P. Allen and D. J. Tildesley, *Computer Simulation of Liquids* (Oxford University Press, 1987).
- ⁶⁴ D. Frenkel and B. Smit, *Understanding Molecular Simulation* (Academic Press, London, 2002).
- ⁶⁵ J. P. K. Doye, A. A. Louis, I.-C. Lin, L. R. Allen, E. G. Noya, A. W. Wilber, H. C. Kok, and R. Lyus, *Phys. Chem. Chem. Phys.* **9**, 2197 (2007).
- ⁶⁶ A. W. Wilber, J. P. K. Doye, A. A. Louis, E. G. Noya, M. A. Miller, and P. Wong, *J. Chem. Phys.* **127**, 085106 (2007).
- ⁶⁷ E. G. Noya, C. Vega, J. P. K. Doye, and A. A. Louis, *J. Chem. Phys.* **127**, 054501 (2007).
- ⁶⁸ R. W. Zwanzig, *J. Chem. Phys.* **22**, 1420 (1954).
- ⁶⁹ M. Parrinello and A. Rahman, *J. Appl. Phys.* **52**, 7182 (1981).
- ⁷⁰ S. Yashonath and C. N. R. Rao, *Mol. Phys.* **54**, 245 (1985).
- ⁷¹ J. L. Aragonés, E. G. Noya, J. L. F. Abascal, and C. Vega, *J. Chem. Phys.* **127**, 154518 (2007).

TABLE I: Free energy of the sc structure of the patchy model particles at $T^* = 0.2$, and of the CP1 structure of hard dumbbells (HD), as obtained using the Einstein molecule and the Einstein crystal methods. For the patchy model we used $\Lambda_E/(k_B T/\sigma_{LJ}^2) = 20000$ and $\Lambda = \sigma_{LJ}$ and for HD $\Lambda_E/(k_B T/\sigma_{HS}^2) = 4000$ and $\Lambda = \sigma_{HS}$.

System	ρ^*	N	Einstein molecule				Einstein crystal			
			$\frac{A_0}{Nk_B T}$	$\frac{\Delta A_1}{Nk_B T}$	$\frac{\Delta A_2}{Nk_B T}$	$\frac{A_{sol}}{Nk_B T}$	$\frac{A_0^*}{Nk_B T}$	$\frac{\Delta A_1^*}{Nk_B T}$	$\frac{\Delta A_2^*}{Nk_B T}$	$\frac{A_{sol}^*}{Nk_B T}$
Patchy (sc)	0.763	125	27.747	-14.614	-14.313	-1.181(7)	27.689	-14.614	-14.256	-1.181(7)
Patchy (sc)	0.763	216	27.792	-14.614	-14.311	-1.134(7)	27.755	-14.614	-14.278	-1.138(7)
HD (CP1)	0.590	144	19.633	0.001	-7.056	12.578(7)	19.580	0.001	-7.005	12.576(7)

TABLE II: Free energies of ices XIII and XIV as calculated using the Einstein crystal and the Einstein molecule methods. The simulation box contained $N = 504$ water molecules for ice XIII and $N = 540$ for ice XIV. Long simulations were performed in order to reduce the statistical error. The maximum value of the coupling parameter was $\frac{\Lambda_E}{k_B T} = 25000 \text{ \AA}^{-2}$ and we used $\Lambda = 1 \text{ \AA}$. The free energy was calculated by performing NVT simulations with the equilibrium simulation box at the studied thermodynamic state, namely, $T=80\text{K}$ and $p=1\text{bar}$.

Ice	$p(\text{bar})$	$T(\text{K})$	$\rho(g/cm^3)$	Einstein molecule				Einstein crystal			
				$\frac{A_0}{Nk_B T}$	$\frac{\Delta A_1}{Nk_B T}$	$\frac{\Delta A_2}{Nk_B T}$	$\frac{A_{sol}}{Nk_B T}$	$\frac{A_0^*}{Nk_B T}$	$\frac{\Delta A_1^*}{Nk_B T}$	$\frac{\Delta A_2^*}{Nk_B T}$	$\frac{A_{sol}^*}{Nk_B T}$
XIII	1	80	1.262	29.491	-91.229	-15.769	-77.508(8)	29.472	-91.229	-15.756	-77.512(8)
XIV	1	80	1.332	29.493	-91.073	-16.259	-77.839(8)	29.475	-91.073	-16.246	-77.843(8)

TABLE III: Free energies of ices XIII and XIV as calculated using the Einstein molecule method. The data marked with an asterisk correspond to calculations of the free energy using a reference structure in which the positions and orientations of the Einstein field are those obtained from simulated annealing up to 1 K, while the data with two asterisks correspond to the structure with the average positions and orientations of the water molecules at the particular thermodynamic state. As can be seen, the free energy does not depend on the choice of the positions and the orientations of the Einstein external field. In all these simulations we have taken $\Lambda = 1 \text{ \AA}$ and $\Lambda_E/(k_B T/\text{\AA}^2) = \Lambda_{E,a}/(k_B T) = \Lambda_{E,b}/(k_B T) = 25000$.

Ice	$p(\text{bar})$	$T(\text{K})$	$\rho(\text{g}/\text{cm}^3)$	$\frac{U}{Nk_B T}$	$\frac{\Lambda_E}{k_B T}(\text{\AA}^{-2})$	$\frac{A_0}{Nk_B T}$	$\frac{\Delta A_1}{Nk_B T}$	$\frac{\Delta A_2}{Nk_B T}$	$\frac{A_{sol}}{Nk_B T}$
XIII	1	80	1.262	-89.08	25000	29.49	-91.23	-15.77	-77.51(4)
XIII*	1	80	1.262	-89.08	25000	29.49	-92.07	-14.94	-77.52(4)
XIII	5000	80	1.294	-89.12	25000	29.49	-91.20	-15.68	-77.39(4)
XIII	1	250	1.208	-26.01	25000	29.49	-28.96	-19.04	-18.51(4)
XIV	1	80	1.332	-89.64	25000	29.49	-91.07	-16.24	-77.82(4)
XIV*	1	80	1.332	-89.64	25000	29.49	-92.61	-14.72	-77.84(4)
XIV**	1	80	1.332	-89.64	25000	29.49	-92.63	-14.69	-77.83(4)
XIV	5000	80	1.360	-89.71	25000	29.49	-91.02	-16.20	-77.73(4)
XIV	1	250	1.271	-26.17	25000	29.49	-28.95	-18.99	-18.45(4)

TABLE IV: Free energies of the patchy model (see Eq. 2) for different values of N and solid structures at $T^* = 0.2$. We also report the value of the three different terms that contribute to $\frac{A_{0,t}}{Nk_B T}$ (see Eq. 9), namely, $\frac{A_{0,t,1}}{Nk_B T} = \ln(\Lambda^3 \rho)/N$, $\frac{A_{0,t,2}}{Nk_B T} = \frac{3}{2} \ln(\Lambda^2 \beta \Lambda_E / \pi)$, $\frac{A_{0,t,3}}{Nk_B T} = -\frac{3}{2N} \ln(\Lambda^2 \beta \Lambda_E / \pi)$. In these calculations we used $\Lambda_E / (k_B T / \sigma_{LJ}^2) = 20000$ and Λ was taken as σ_{LJ} .

System	ρ^*	N	$\frac{A_{0,t,1}}{Nk_B T}$	$\frac{A_{0,t,2}}{Nk_B T}$	$\frac{A_{0,t,3}}{Nk_B T}$	$\frac{A_{0,or}}{Nk_B T}$	$\frac{A_0}{Nk_B T}$	$\frac{\Delta A_1}{Nk_B T}$	$\frac{\Delta A_{2,t}}{Nk_B T}$	$\frac{\Delta A_{2,or}}{Nk_B T}$	$\frac{A_{sol}}{Nk_B T}$
Patchy (sc)	0.763	125	-0.002	13.138	-0.105	14.716	27.746	-14.614	-5.731	-8.583	-1.181
Patchy (sc)	0.763	216	-0.001	13.138	-0.061	14.716	27.792	-14.614	-5.728	-8.583	-1.134
Patchy (sc)	0.763	512	-0.001	13.138	-0.026	14.716	27.828	-14.614	-5.729	-8.582	-1.097
Patchy (sc)	0.763	1000	-0.000	13.138	-0.013	14.716	27.840	-14.614	-5.729	-8.581	-1.084
Patchy (bcc)	1.175	250	0.001	13.138	-0.053	14.716	27.802	-13.718	-5.231	-8.562	0.291
Patchy (bcc)	1.175	432	0.000	13.138	-0.030	14.716	27.824	-13.718	-5.236	-8.564	0.306
Patchy (bcc)	1.175	1024	0.000	13.138	-0.013	14.716	27.841	-13.718	-5.241	-8.567	0.315
Patchy (fcc)	1.360	256	0.001	13.138	-0.051	14.716	27.804	-6.193	-2.912	-10.108	8.591
Patchy (fcc)	1.360	500	0.001	13.138	-0.026	14.716	27.828	-6.192	-2.913	-10.109	8.614
Patchy (fcc)	1.360	864	0.000	13.138	-0.015	14.716	27.839	-6.190	-2.915	-10.111	8.623

TABLE V: Value of the different terms that contribute to the free energy of the LJ fcc solid at $\rho^* = 1.28$ and $T^* = 2.0$. The LJ potential was truncated at $2.7\sigma_{LJ}$. Long range corrections (assuming that $g(r)=1$ beyond the cutoff) have been added. We also report the value of the three different terms that contribute to $\frac{A_{0,t}}{Nk_B T}$, namely, $\frac{A_{0,t,1}}{Nk_B T} = \ln(\Lambda^3 \rho)/N$, $\frac{A_{0,t,2}}{Nk_B T} = \frac{3}{2} \ln(\Lambda^2 \beta \Lambda_E / \pi)$, $\frac{A_{0,t,3}}{Nk_B T} = -\frac{3}{2N} \ln(\Lambda^2 \beta \Lambda_E / \pi)$. The free energy calculations were performed using a maximum value of the coupling parameter $\Lambda_E / (k_B T / \sigma_{LJ}^2) = 14000$. Λ was taken as σ_{LJ} .

N	$\frac{A_{0,t,1}}{Nk_B T}$	$\frac{A_{0,t,2}}{Nk_B T}$	$\frac{A_{0,t,3}}{Nk_B T}$	$\frac{A_0}{Nk_B T}$	$\frac{\Delta A_1}{Nk_B T}$	$\frac{\Delta A_2}{Nk_B T}$	$\frac{A_{sol}}{Nk_B T}$
256	0.001	12.603	-0.049	12.555	-3.620	-6.365	2.570
500	0.000	12.603	-0.025	12.578	-3.620	-6.372	2.586
864	0.000	12.603	-0.015	12.589	-3.620	-6.377	2.592
1372	0.000	12.603	-0.009	12.594	-3.620	-6.380	2.594

TABLE VI: Free energies of the sc, bcc, and oriented fcc crystals for the octahedral patchy model at $T^* = 0.2$ and for the LJ model at $T^* = 2.0$ including finite size corrections (FSC). No FSC corrections means the true free energy for the system of size N .

System	ρ^*	N	$A/(NkT)$						
			No FSC	FSC-HS2	FSC-FL	FSC-HS	FSC-as1	FSC-as2	FSC-as3
Patchy (sc)	0.763	125	-1.181	-1.123	-1.104	-1.125	-1.074	-1.120	-1.097
Patchy (sc)	0.763	216	-1.134	-1.096	-1.084	-1.101	-1.071	-1.098	-1.085
Patchy (sc)	0.763	512	-1.097	-1.079	-1.073	-1.083	-1.071	-1.082	-1.076
Patchy (sc)	0.763	1000	-1.084	-1.073	-1.070	-1.077	-1.070	-1.076	-1.073
Patchy (sc)	0.763	∞	-1.069	-1.069	-1.069	-1.069	-1.069	-1.069	-1.069
Patchy (bcc)	1.175	250	0.291	0.324	0.335	0.319	0.343	0.322	0.332
Patchy (bcc)	1.175	432	0.306	0.327	0.334	0.322	0.336	0.324	0.330
Patchy (bcc)	1.175	1024	0.315	0.325	0.328	0.322	0.328	0.322	0.325
Patchy (bcc)	1.175	∞	0.324	0.324	0.324	0.324	0.324	0.324	0.324
Patchy (fcc)	1.360	256	8.591	8.623	8.634	8.618	8.641	8.629	8.635
Patchy (fcc)	1.360	500	8.614	8.633	8.639	8.628	8.640	8.634	8.637
Patchy (fcc)	1.360	864	8.623	8.634	8.638	8.631	8.638	8.634	8.636
Patchy (fcc)	1.360	∞	8.637	8.637	8.637	8.637	8.637	8.637	8.637
LJ	1.28	256	2.570	2.602	2.613	2.597	2.618	2.593	2.606
LJ	1.28	500	2.586	2.605	2.611	2.600	2.611	2.598	2.604
LJ	1.28	864	2.592	2.604	2.608	2.600	2.606	2.599	2.603
LJ	1.28	1372	2.594	2.602	2.605	2.599	2.603	2.598	2.601
LJ	1.28	∞	2.601	2.601	2.601	2.601	2.601	2.601	2.601

TABLE VII: Performance of the different FSC. Deviation of the corrected values of the free energy at a given N from the value at the thermodynamic limit ($d = \frac{A_{sol}(N)}{Nk_B T} - \frac{A(N=\infty)}{Nk_B T}$). For the solids studied in this work we computed the mean deviation for the smallest size studied, while for the HS solid it was estimated for $N = 256$. The mean deviation for each FSC is also provided (computed as $\bar{d} = \sum |d|/n \times 10^3$).

System	ρ^*	No FSC	FSC-HS2	FSC-FL	FSC-HS	FSC-A1	FSC-A2	FSC-A3
HS	1.04086	-0.028	0.004	0.016	0.000	0.003	-0.009	-0.003
HS	1.099975	-0.030	0.002	0.013	-0.003	0.007	-0.008	0.000
HS	1.1500	-0.034	-0.002	0.009	-0.007	0.002	-0.010	-0.004
LJ	1.2800	-0.031	0.001	0.012	-0.004	0.017	-0.008	0.005
Patchy (sc)	0.763	-0.112	-0.054	-0.035	-0.056	-0.005	-0.051	-0.028
Patchy (bcc)	1.175	-0.033	0.000	0.011	-0.005	0.019	-0.002	0.008
Patchy (fcc)	1.360	-0.046	-0.014	-0.003	-0.019	0.004	-0.008	-0.002
\bar{d}		55	11	14	13	8	14	7

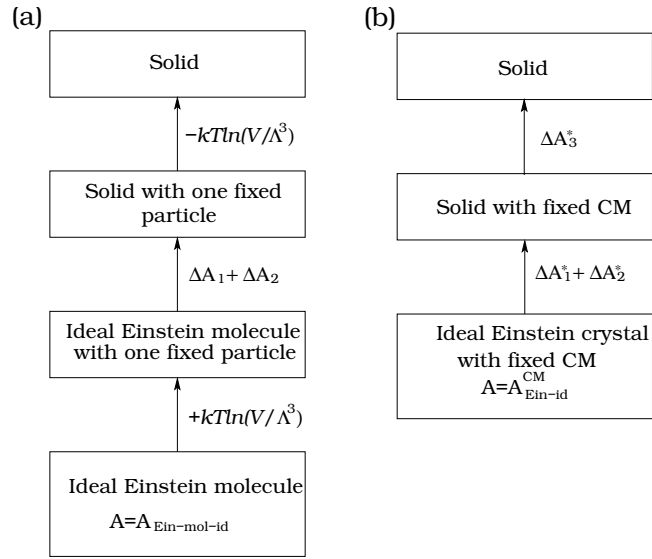


FIG. 1: Thermodynamic path used in (a) the Einstein molecule approach^{37,38} and (b) the Einstein crystal method.^{2,39}

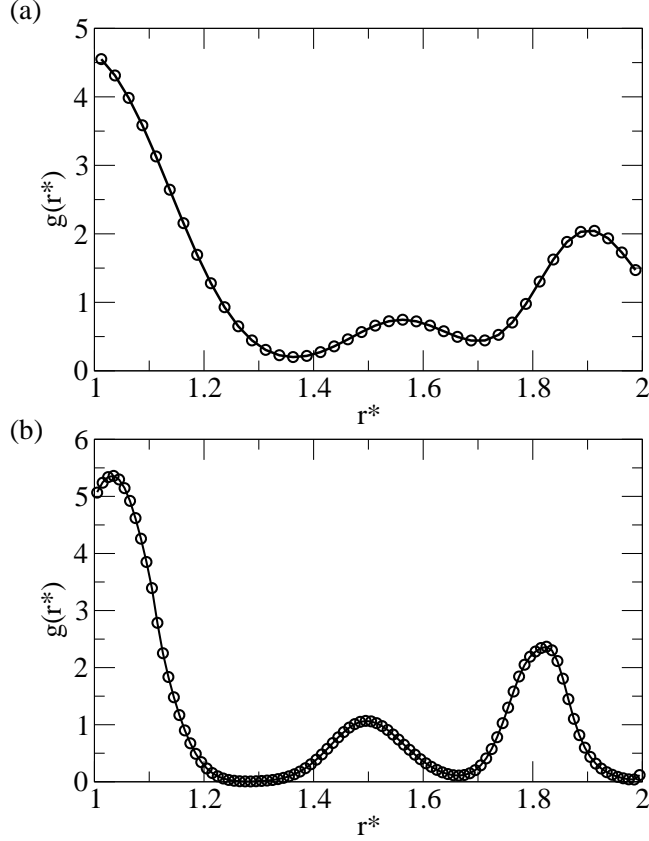


FIG. 2: (a) Radial distribution function for hard spheres in the fcc solid phases when particle 1 moves (solid line) and when it does not move (open circles). Results correspond to $\rho^* = 1.04086$ for a system size $N = 108$. (b) Site-site radial distribution function for hard-dumbbells with $L^* = 1$ in the CP1 structure at $\rho^* = 0.590$ and for a system size $N = 32$ when molecule 1 moves (solid line) and when the reference point of molecule 1 (i.e., its center of mass) is fixed but molecule 1 can rotate (open circles). As can be seen, the structural properties are the same, illustrating that the properties of the solid present translational invariance.

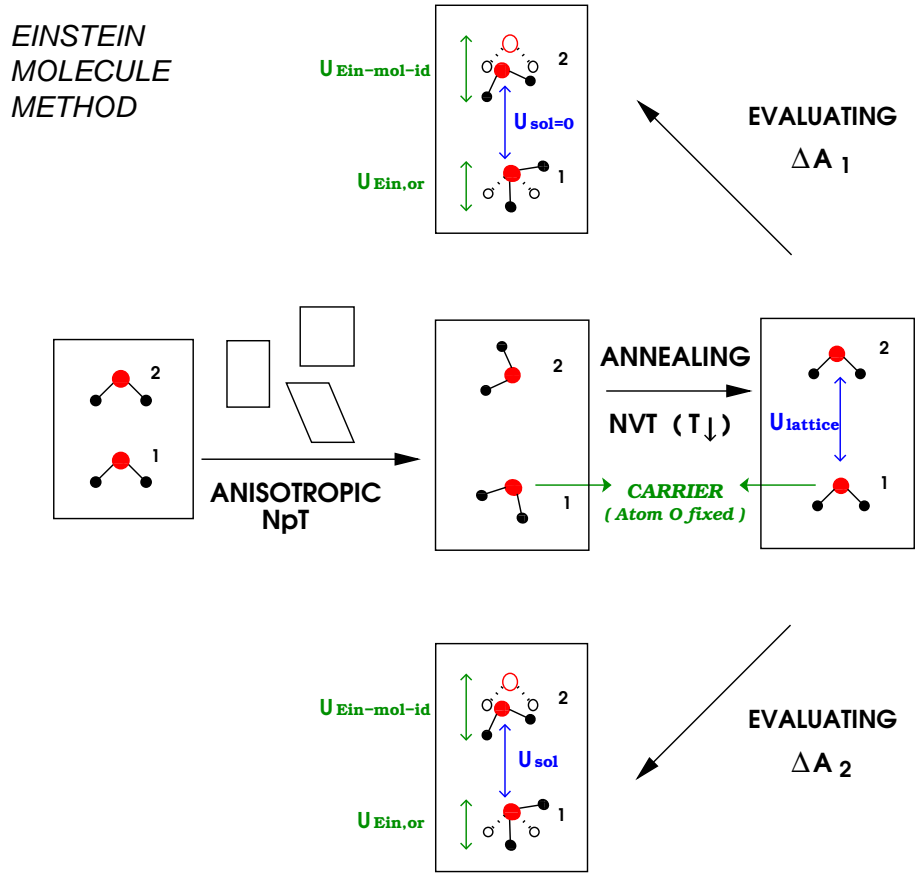


FIG. 3: Schematic representation of the procedure to compute the free energy of molecular solids by the Einstein molecule approach. In the first stage a Parrinello-Rahman NpT simulation is carried out to obtain the equilibrium shape of the simulation box at the thermodynamic state under study. Second, starting from a configuration with the equilibrium shape of the simulation box, the position and orientations of the molecules in the lowest energy configuration are obtained by simulated annealing (the shape of the simulation box is kept constant during the quenching). In order to avoid translations of the system as a whole, the position of the reference point of molecule 1 is kept fixed during the annealing. The final configuration obtained from this quenching, whose energy is $U_{lattice}$, is then used as the reference structure for the computation of the free energy (i.e., for the evaluation of terms ΔA_1 and ΔA_2). As described in the text, it is also possible to take the structure from the experimental value of the coordinates of the molecules or from the average positions. To compute the term ΔA_1 , an NVT simulation of the ideal Einstein molecule (i.e., with the position of the reference point of molecule 1 fixed) is performed, along which the term $\exp[-\beta(U_{sol} - U_{lattice})]$ is averaged, so that ΔA_1 can be computed from Eq. 10. As with regard to the term ΔA_2 , several NVT simulations are performed where both the intermolecular potential and the Einstein field (for different values of the coupling parameter Λ') are present, in which again molecule 1 is not allowed to translate. For each value of the coupling parameter, the

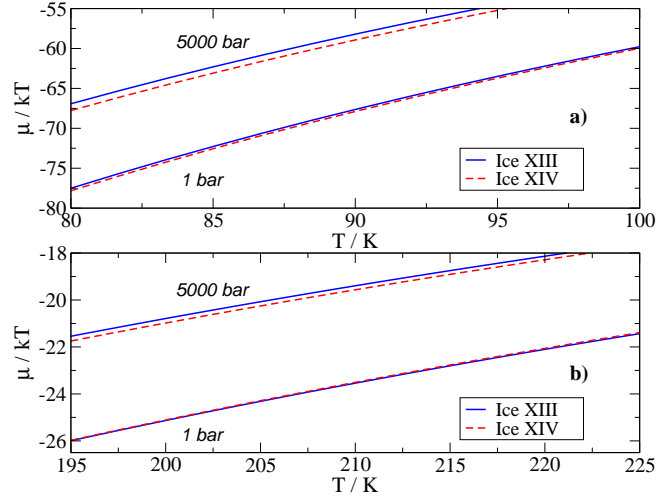


FIG. 4: (a) Chemical potential versus temperature for ices XIII and XIV along the isobars $p=1\text{bar}$ and $p=5000\text{bar}$ at low temperatures. (b) The same as (a) but at temperatures close to the melting point of the model.

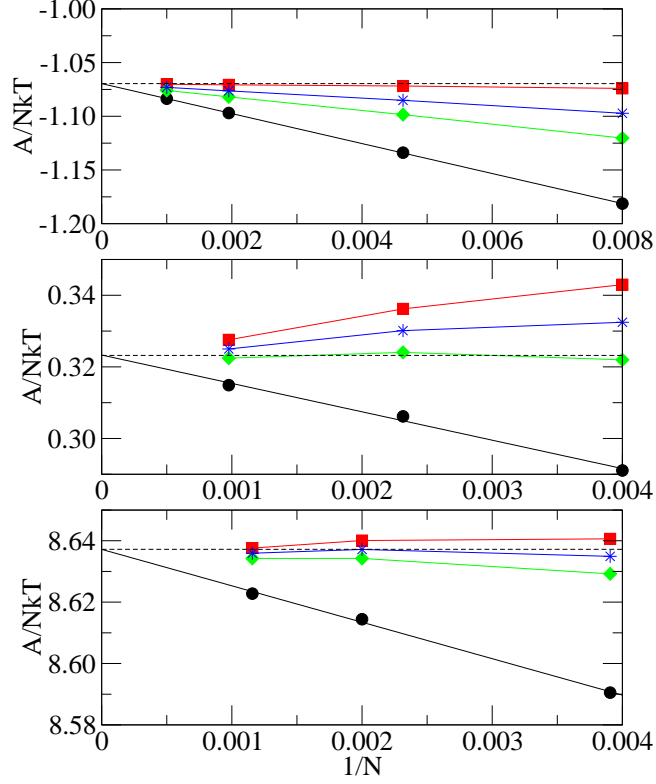


FIG. 5: (Colour online) Size dependence of the free energy of the sc (upper panel), bcc (middle panel) and fcc (bottom panel) solid structures of the six-patches octahedral model. Black circles correspond to the true free energy of the system of size N without any FSC correction and the black line is a linear fit to these points. The black dashed-lines signals the value of the free energy in the thermodynamic limit, obtained from the fit. The red squares correspond to the free energy corrected with the FSC-as1, the green diamonds are the free energy corrected with the FSC-as2 and the blue stars are the values corrected with the FSC-as3. The red, green and blue lines are only a guide to the eyes.